Impact of Source to Substrate Distance on the Properties of Thermally Evaporated CdS Film

Maitry Dey*‡, N. K. Das*, Mrinmoy Dey*, S. F. U. Farhad**, M. A. Matin* and N. Amin***

*Department of Electrical and Electronic Engineering, Chittagong University of Engineering and Technology, Chittagong-4349, Bangladesh

** Industrial Physics Division, Bangladesh Council of Scientific and Industrial Research, Dhaka-1205, Bangladesh

*** Institute of Sustainable Energy, Universiti Tenaga Nasional (@The Energy University), 43000 Kajang, Selangor, Malaysia

(maitrydeyeee@gmail.com, nipudas@cuet.ac.bd, mrinmoy@cuet.ac.bd, imamatin@yahoo.com, nowshad@uniten.edu.my)

‡ Corresponding Author; Maitry Dey, Department of Electrical and Electronic Engineering, Chittagong University of Engineering and Technology, Chittagong-4349, Bangladesh, Tel: +880-1704-920709, maitrydeyeee@gmail.com

Received: 11.12.2020 Accepted:03.02.2021

Abstract- In this work, we present the effect of varying distances between source and substrate of the thermal evaporator on the structural, optical, and electrical properties of as-deposited Cadmium Sulfide thin-films. The CdS films were deposited on the borosilicate glass substrate using the thermal evaporation method under high vacuum conditions to optimize SSD. The variation of SSD greatly influences the physical properties of as-deposited CdS films caused the change in substrate temperature and density of incident adatoms of CdS. The structural and optical properties of as-deposited CdS films were analyzed by X-ray diffraction and UV-VIS-NIR spectroscopy. The Hall Effect Measurement System investigated the three main electrical properties (carrier concentration, carrier mobility, and resistivity) of the deposited CdS films. The XRD pattern of all the CdS thin-films exhibited the polycrystalline nature with the preferential hexagonal (002) plane. The CdS films deposited at 10 cm SSD showed better crystallographic properties among all the deposited films. The optical bandgap of the CdS films followed a decreasing trend from 2.44 eV to 2.37 eV as the SSD decreases from 14 cm to 8 cm due to the improvement of crystallinity of the deposited films. All the deposited CdS films showed the n-type property, and the carrier concentration of the CdS films increases from 3.78×10^{13} cm^{-3} to 4.41×10^{16} cm^{-3} as we decrease the SSD from 14 cm to 8 cm. The CdS films resistivity also decrease with the reduction of SSD. The characterization results suggest that the CdS films deposited at 10 cm SSD are suitable for photonic and thin-films solar cells.

Keywords Thin film; CdS; Thermal Evaporation; Source to Substrate Distance; XRD; UV-VIS-NIR; HEMS.

1. Introduction

The polycrystalline CdS is regarded as one of the potential Photovoltaic (PV) materials that have been extensively explored in the last few decades [1]. The binary (II-VI) semiconductor CdS material is a preference for solar PV applications [2]. The CdS material gets n-type conductivity because of its Sulfur (S) vacancies, V_s during the processing [1, 2]. Typically donor concentration of processed CdS thin-film is about $10^{16} \sim 10^{17}$ cm^{-3} [3]. It exhibits a high absorption coefficient *(α)* is approximately $(2.29 – 4.93)\times10^5$/cm [4] which occurs especially in the short wavelength region beneath 510 nm [5, 6]. Moreover, it has a direct bandgap of 2.42 eV [7, 8], high transparency [9], and high absorption but in the blue region [10]. The mentioned attractive optoelectronic properties make CdS material as a suitable window layer for thin-film PV solar cells [11, 12] and optoelectronic devices [13, 14].

Many researchers are doing intensive research work to improve the quality of the film for various applications. Meanwhile, the low-cost fabrication methods for synthesizing the CdS material make it attractive. In particular, within the last few years, more than ten methods have been used to deposit the CdS thin films [15]. Above these methods, Close-Spaced Sublimation (CSS) [16], Chemical Bath Deposition (CBD) [17], RF and DC Sputtering [18], Spray Pyrolysis [19], Pulsed Laser Deposition (PLD) [20], Sol-Gel [21], Thermal Evaporation (TE) [22], and Electrode Deposition [23] are mostly used for CdS film synthesis. Each method has different deposition parameters needed to optimize the deposition recipe to obtain better as-grown film

characteristics. The TE method is frequently used to prepare high-quality films in the semiconductor industry, such as CdS, CdTe, etc. The TE is a high vacuum thin film deposition method widely used to deposit the nano-structured film and permit a uniform, homogeneous, and better crystallinity over the substrates' enormous territory [22]. For that reason, this method is preferred for synthesizing the CdS thin film in this work.

The as-deposited film's physical properties in the TE method depend on the different process parameters like substrate temperature, pressure, substrate material, and SSD. It is well known that the as-deposited CdS thin films comprise many phases such as cubic, hexagonal, or both mix phases due to their deposition condition. The effect of substrate temperature and process ambient of TE on the crystallographic and optical properties of CdS thin films was reported in previously published works [24, 25]. In 2007 Devika et al. reported that the distance between the source and the substrate influence the SnS thin films grain size, roughness, thickness, and percentage ratio of Sn and S of the deposited SnS films decreased [26]. In another study, Kai et al. studied the effect of the distance between the substrate and the evaporation source to find the Be films' physical properties since the SSD is a function of substrate temperature and the adatoms kinetic energy [27]. To the best of our knowledge, no reports on TE deposited CdS film for variable SSD. Hence, SSD effects on the CdS films are investigated to explore the optimum growing condition for better performance. Subsequently, it creates an increased interest in studying the SSD's effect on thermally evaporated CdS films' physical properties.

In this work, the CdS thin films were grown on BSG substrates for different evaporation source to substrate distance by using VCM 600 V1 thermal evaporator machine to observe the influence of SSD on the structural, optical, and electrical properties of the as-deposited CdS thin films.

2. Experimental Details

2.1. *Substrate Preparation of CdS Thin Film*

Initially, the bare BSGs were scratched by a diamond pen cutter on one side of all substrates to identify the deposited sides. Both sides of substrates were mechanically scribed by a clean brush in a glass beaker containing soapy water for two minutes of each side and then rinsed with deionized (DI) water. After mechanical scribing, these substrates were cleaned sequentially by MAMD (MAMD stands for the introduction of Methanol, Acetone, and then again Methanol and Deionized water solution) process in an ultrasonic bath [28, 29].

During the cleaning procedure in the ultrasonic bath, each step lasted for 10 minutes with methanol, acetone, and again methanol solution while 15 minutes for DI water at 50 ˚C temperature. These wet substrates were dried by pure industrial nitrogen (N_2) gas and further baked-on hot-plate at 100 ˚C for 5 minutes. The substrate holder, evaporation boat, and growth chamber of the thermal evaporator machine were carefully wiped out with ethanol-soaked lint-free tissues. Later, we attached the clean BSG substrate to the cleaned substrate holder and placed it inside the TE chamber.

2.2. *Deposition of CdS Thin Film*

The CdS thin films were prepared onto clean glass substrates by the TE method. We used high purity (99.999%) CdS powder as source material for VCM 600 V1 thermal evaporator machine, and it was evaporated by a Molybdenum (Mo) evaporation boat. The experimental setup of VCM 600 V1 TE machine and its growth chamber shown in Fig. 1 during the deposition of CdS films.

Fig. 1. Full set up of Thermal Evaporator machine in CUET.

Before the evaporation, the TE chamber was pump-down to 10^{-6} hPa by a turbomolecular pump. After that, gradually increased the evaporation boat current to 160 A AC for evaporating the CdS thin films for 3 minutes in all experiments. The CdS thin films were deposited onto the glass substrate for four different SSD (Δd): 8 cm (CdS_S4), 10 cm (CdS_S3), 12 cm (CdS_S2), and 14 cm (CdS_S1) while keeping the other process parameters of the TE constant. The CdS film deposition recipe used in this work took from the related published papers after reasonable estimation [25, 28, 30]. The growth parameters of VCM 600 V1 thermal evaporator for CdS synthesis are given in Table 1.

Table 1. Deposition parameters of CdS window layer.

Process Parameter	Value
Evaporation Boat	Molybdenum
Chamber Pressure	10^{-6} hPa
Deposition Current	160 A
Deposition Time	3 minutes
SSD	14, 12, 10, 8 cm

After the CdS film evaporation had been completed, the deposition current gradually decreased to zero amperes and allowed time to cool down the samples and evaporation boat.

2.3 *Characterization of CdS Thin Film*

The Dektak profilometer measured the thickness of the as-deposited CdS films, and the deposited thickness is around 200 nm. As-grown CdS film is shown in Fig. 2. A vacuum desiccator was used to preserve the thermally evaporated CdS film samples to avoid any film quality deterioration before the characterization.

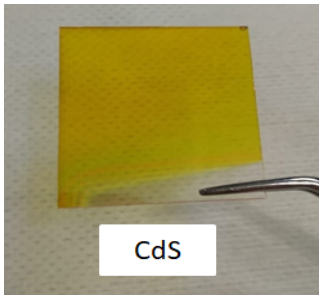

Fig. 2. Thermally evaporated CdS film on BSG.

The electrical properties of thermally evaporated CdS films were investigated using ECOPIA Hall Effect Measurement System (HEMS 3000) integrated by a resistivity/ Hall measurement tool. The structural analysis of all the CdS films was carried out by the "BRUKER aXS-D8" diffractometer whose "Cu-Kα" X-ray radiation wavelength, λ = 0.15406 nm. All thermally evaporated CdS films were investigated for optical analysis by SHIMADZU UV-2600 spectrophotometer for a wavelength range of 200 - 1100 nm.

3. Results and Discussion

3.1 *Structural Properties of CdS Thin FIlm*

The XRD patterns of the as-deposited CdS films at various SSD of 8, 10, 12, and 14 cm are presented in Fig. 3. The diffraction patterns were recorded in intervals from 20 up to 80 with a 2°/min scanning rate.

All the as-deposited CdS films exhibited polycrystalline nature and suggested that the hexagonal wurtzite structure with a very sharp prominent peak at 2θ = 26.4° corresponding to the (002) plane shown in Fig. 3.

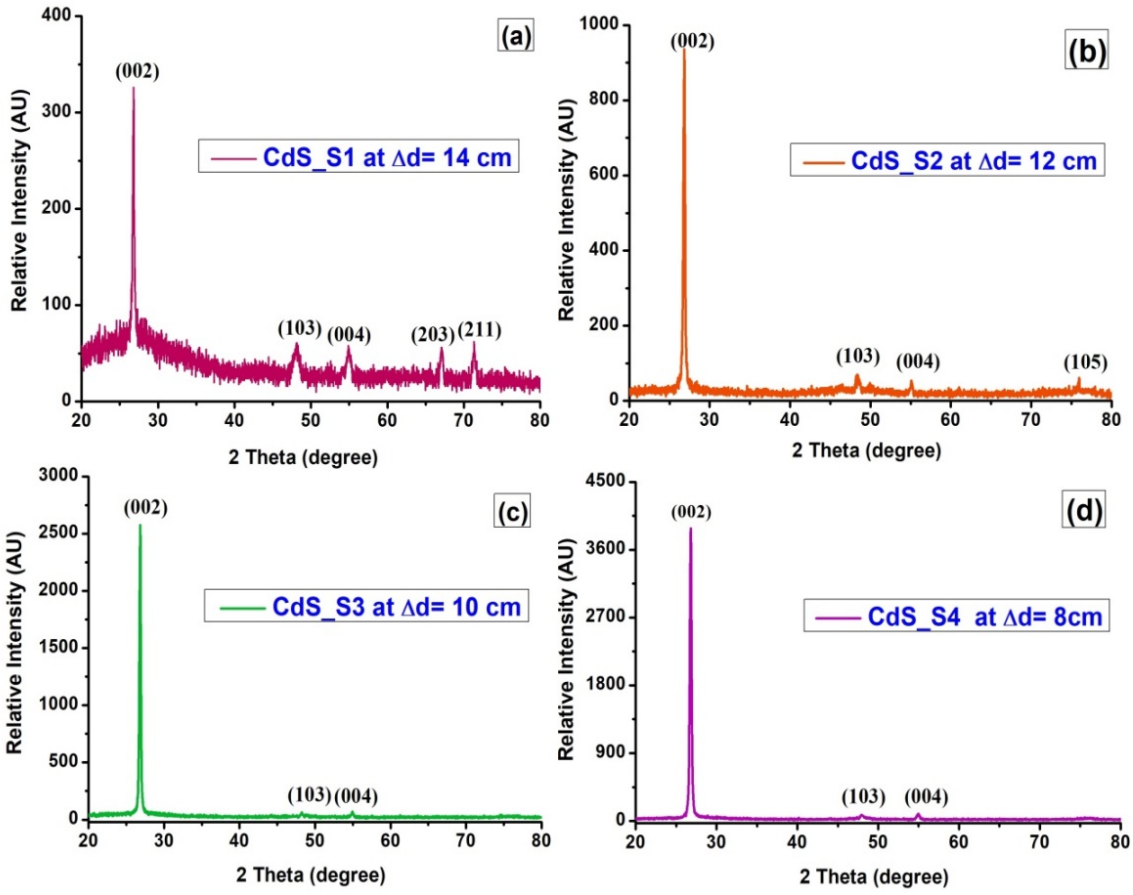

Fig. 3. XRD pattern of the thermally evaporated CdS films

The hexagonal wurtzite crystal structure of CdS films oriented at (002) is more stable than the cubic zinc blend structure and prefers the solar cell application of that advantage [31].

It is observed in Fig. 3 (a) that the thermally evaporated CdS_S1 sample deposited at SSD of 14 cm has four minor peaks corresponding to (103), (004), (203), and (211) are found at 2θ ≈ 48.1°, 54.9°, 67.12°, and 71.31° intensity respectively. As the SSD decreases from 14 cm to 8 cm, the minor peaks corresponding to (203), (211), and (105) planes disappeared due to a reduction in the microstrain, dislocations, and lattice misfits from these planes [32]. Fig. 4 illustrates the variation of the (002) plane's prominent peak intensity with the SSD for better understand.

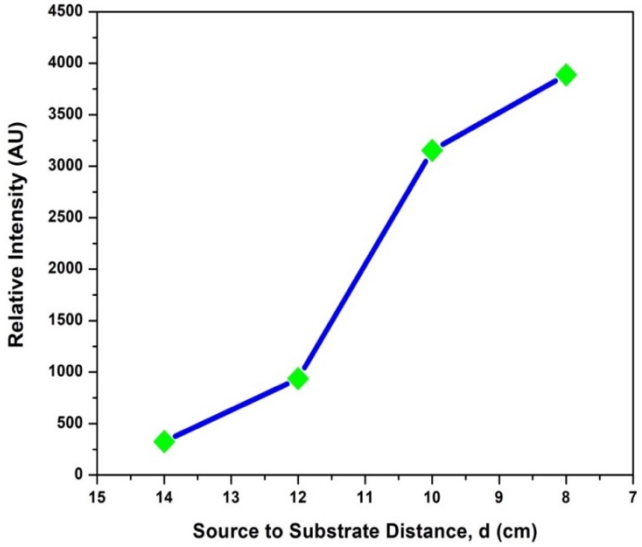

Fig. 4. Highest peak intensity of (002) plane for CdS films grown at different SSD.

The variation of the lattice constant, crystallite size, micro-strain, and dislocation density, and the peak intensity in the thermally evaporated CdS film samples occurs due to the growth distance presented in Table 2. These structural properties have been calculated from the dominant peak of the XRD pattern. The lattice constant for the hexagonal plane of the CdS films is determined by Brag's law and Vegard's law [29]:

$$d_{hkl} = \left(\frac{\lambda}{2}\right)\cos ec\theta \tag{1}$$

$$a_{hexagonal} = d_{hkl}\sqrt{h^2 + k^2 + l^2}\sqrt{0.5} \tag{2}$$

$$c_{hexagonal} = d_{hkl}\sqrt{h^2 + k^2 + l^2}\sqrt{(\frac{4}{3})} \tag{3}$$

Where d_{hkl} represents the interplanar spacing in the crystal in which λ is the X-ray wavelength equal to 0.15406 nm, θ refers to the angle between the incident X-ray and the scattering plane.

Scherrer equations (4-6) are applied to determine the crystallite size D, micro-strain ε, and dislocation density δ for the CdS thin films as assigned in Table 2 [29, 32]:

$$D_{hkl} = \frac{0.9\lambda}{\beta\cos\theta} \tag{4}$$

$$\varepsilon = \frac{\beta}{4\tan\theta} \tag{5}$$

$$\delta = \frac{n}{D^2} \tag{6}$$

Where λ is the X-ray wavelength (0.15406 nm), θ is the Bragg's angle, and β is the full width at half maximum [FWHM] of the most intense peak (002), and n is considered a unity factor for minimum dislocation density.

It is evident from the crystallographic data in Table 2 that the crystallite size increased with SSD decreases up to 10 cm. In contrast, micro-strain and dislocation density decreases, and afterward, properties are decreased at 8 cm. The reduction of SSD increases the substrate temperature, which helps the deposited films' recrystallization. Consequently, it enhanced the crystallite size, and this study

Table 2. Calculated values of structural properties of thermally evaporated CdS thin-films.

Sample	SSD, Δd (cm)	Lattice Constant		Crystallite Size, D (nm)	Micro Strain, ε ($\times10^{-3}$)	Dislocation Density, δ ($\times10^{11}$ cm^{-2})
		a (Å)	c (Å)			
CdS_S1	14 cm	4.138	6.746	27.486	5.44	1.32
CdS_S2	12 cm	4.133	6.736	34.346	4.35	0.85
CdS_S3	10 cm	4.133	6.736	37.779	3.95	0.70
CdS_S4	8 cm	4.337	6.738	32.435	4.61	0.95

is consistent with previous reports [25-27, 33]. The smallest crystallite size at 8 cm distance may be due to excess kinetic energy and higher substrate temperature induced by the higher surface migration of CdS atoms [25-27]. The deposited CdS film at 10 cm SSD demonstrates a better crystallinity with a sharp dominant peak intensity of the (002) plane than the other distances deposited films because of the proper orientation along the (002) plane. The lattice constant data of the CdS films are almost matched with the standard lattice constant values (a ~ 4.137 Å, c ~ 6.716 Å) that confirm the deposited CdS films are hexagonal type depicted in Table 2. The estimated values of crystallite size, microstrain, etc., are in good agreement with the related published works [24, 34, 35].

3.2 *Optical Properties of CdS Thin FIlm*

The optical transmission and absorbance spectrum of thermally evaporated CdS films grown on the BSG substrates at different SSD were measured for wavelength 200 - 1100 nm, as illustrated in Fig. 5. The transmittance spectrum of all CdS films revealed the interference fringe pattern with a sudden fall that happened near the band edge.

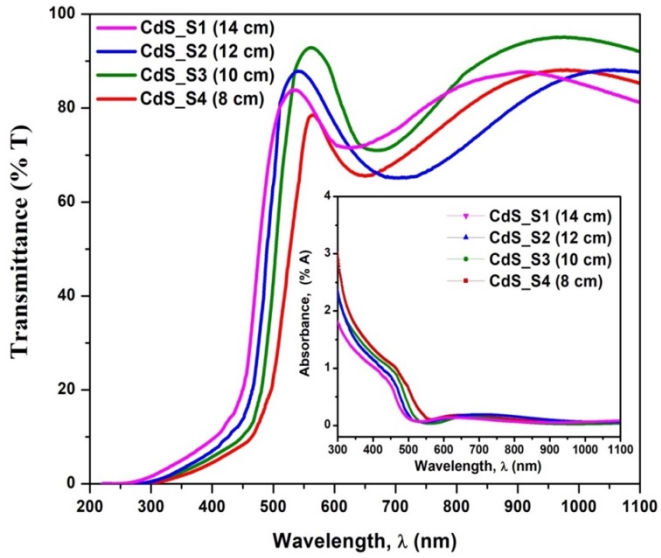

Fig. 5. The transmission spectrum of all the thermally evaporated CdS thin films. (Insert) Image of absorbance spectrum of those films.

It appears a sharp fall in the optical transmission near the fundamental absorption regions of CdS film samples with SSD decrement. It may be due to the recrystallization of the film and an increase in the crystallite size. The transmission spectrum edges of all CdS films started near about 300 nm wavelengths. The transmission spectrum showed an average transmittance of over 75% after 500 nm wavelengths, suitable for the application as a window layer for thin-film solar cells. A significant increment in the transmittance on the short wavelength region (~ 350 - 500 nm) is observed for the thermally evaporated CdS thin films, which improved the blue response.

This property is desirable as a window layer since it allows more photons to pass through the absorber layer and increase the photogenerated carriers. Moreover, the absorption spectrum edges for all thermally evaporated CdS thin films are laid in the wavelength range between 400 nm to 500 nm. The absorption coefficient tends to decrease with the decreases in the SSD of the thermal evaporator chamber.

For the entire absorption region, the absorption coefficient, α was computed from the transmission data using the following relation [29]:

$$\alpha = 1/t \ \ln[(1-R)^2 / T] \tag{7}$$

T, R, and t indicate the transmission, reflection, and thickness of the thermally evaporated CdS. The optical spectrum (transmission and absorbance) is shown in Fig. 5, which means that the thermally evaporated CdS films have comparatively low absorption and better transmission, which is agreeable with previously reported works [24, 35-37]. These results also assure that all deposited CdS samples are suitable for the window layer material for applying the solar cell.

The bandgap was computed for all thermally evaporated CdS films using the Tauc's relation, where the absorption coefficient is related to the bandgap [29].

$$\alpha h\nu = \frac{A(h\nu - Eg)^{n=\frac{1}{2}}}{h\nu} \tag{8}$$

Where A is the energy constant, hv, and Eg refers to the incident photon's energy and bandgap of the material. As the CdS material allowed the direct transition hence the magnitude of n is 1/2. Using the Tauc's relation, the graph of $(\alpha hv)^2$ versus photon energy (hv) for thermally evaporated CdS films at different SSD is plotted, shown in Fig. 6. The optical bandgap of CdS films is obtained through the extrapolating of the linear part in the graph.

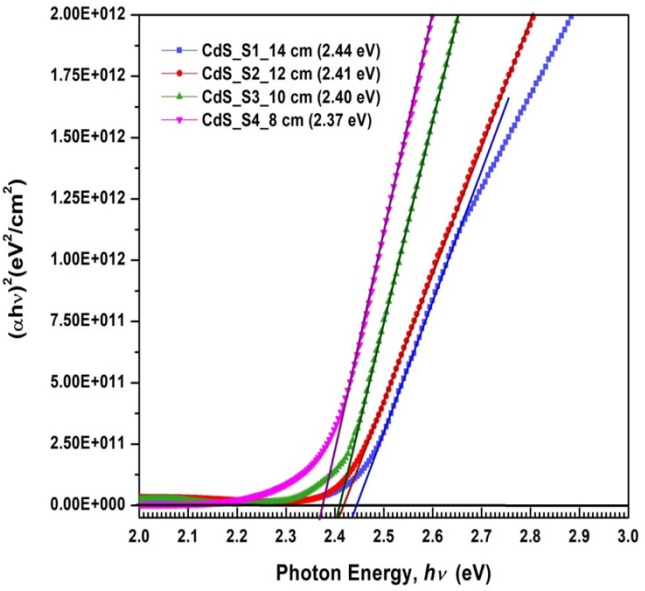

Fig. 6. Optical bandgap of thermally evaporated CdS films at different SSD.

The optical bandgap for CdS films is estimated to be 2.37 eV, 2.40 eV, 2.41 eV, and 2.44 eV with an SSD of 8 cm, 10 cm, 12 cm, and 14 cm, respectively. The lowest and highest bandgap are found for the sample CdS_S4 and sample CdS_S1, respectively. It is conspicuous that the bandgap of thermally evaporated CdS films decreased slightly with the decreases in SSD. This above event occurs due to the crystallite size increment [27, 38, 39]. These bandgap values for all thermally evaporated CdS film samples are close to 2.42 eV that agree with related works [33, 36].

3.3. *Electrical Properties of CdS Thin Film*

The parameters, like carrier concentration, mobility, and resistivity, are mainly examined to evaluate a deposited film's electrical properties. This measurement was performed by applying a constant current source and magnetic field with 36 nA and 0.5 T, respectively, in this ECOPIA HEMS 3000. All the thermally evaporated CdS films showed n-type property. A variety of carrier concentrations (n) is observed for as-grown CdS films as we change SSD from 14 cm to 8 cm, and this phenomenon is illustrated in Fig. 7. The carrier concentration increases from 3.78×10^{13} cm^{-3} to 4.4×10^{16} cm^{-3} as we decrease the SSD from 14 cm to 8 cm.

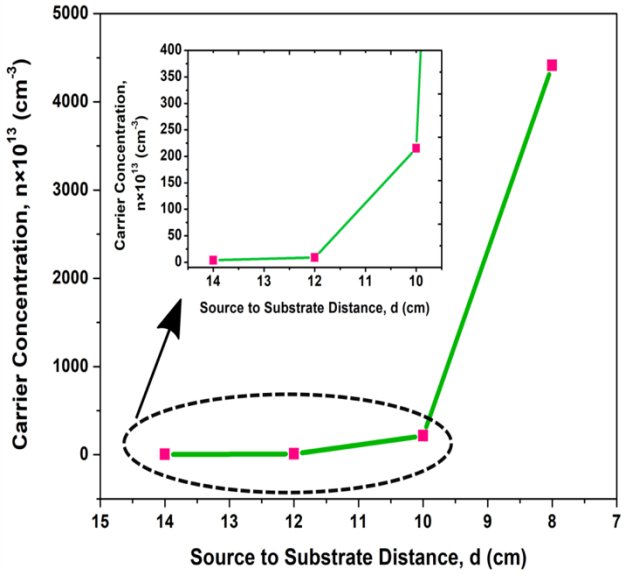

Fig. 7. Carrier concentration of as-deposited CdS films with SSD.

It is observed from Fig 7. that the carrier concentration of deposited CdS thin films increases with the decreases in SSD due to increment in the ratio of Cadmium (Cd) than the Sulfide (S) atom in the interstitial defect densities. These may occur for decreasing SSD where substrate temperature increases and kinetic energy of the evaporated particles, particularly for S atoms, is high because of their high vapor pressure. These S atoms diffused from the hot substrate resulting in a Sulfur deficiency occurred in the deposited films. The sharply increased carrier density from 2.15×10^{15} cm^{-3} to 4.4×10^{16} cm^{-3} as we were changed the SSD from 10 cm to 8 cm may cause higher substrate temperature and S atoms' excessive kinetic energy [25-27, 39].

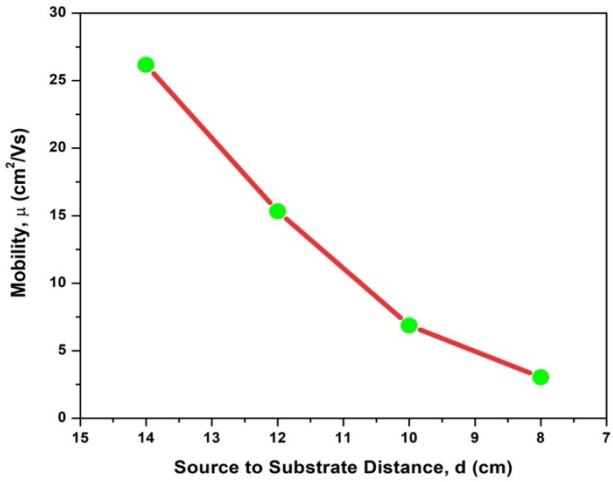

Fig. 8. Carrier mobility measurement with the variation of SSD.

From Fig. 8, it is apparent that the carrier mobility of the deposited CdS films at 14 cm, 12 cm, 10 cm, and 8 cm is estimated to 26.17 cm^2/Vs, 15.32 cm^2/Vs, 6.87 cm^2/Vs, and 3.03 cm^2/Vs, respectively. It is observed that the carrier mobility of deposited CdS films decreases significantly with the decreases in the SSD. This phenomenon occurs because the mean free path of evaporated CdS atoms is smaller than the distance between source and substrate, and particles would collide with each other, resulting in decreasing the carrier mobility. The decrement in carrier mobility with the decline of SSD is consistent with related published work [40].

The variation in film resistivity, ρ with the change of SSD is presented in Fig. 9.

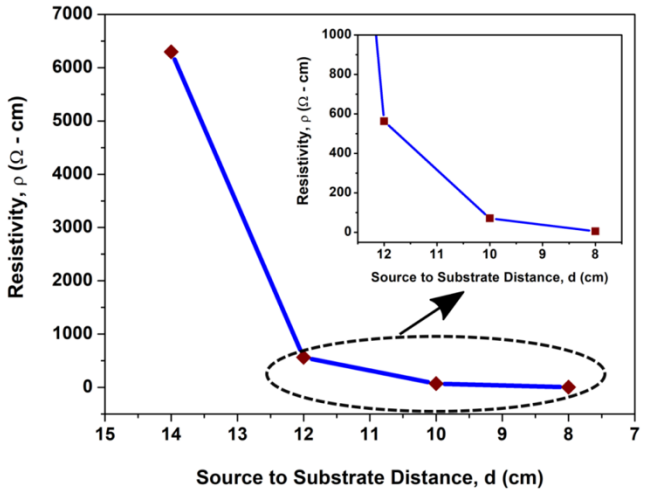

Fig. 9. Film resistivity measurement with the variation of SSD.

As seen in Fig. 9, the resistivity sharply decreases from 10^3 Ω-cm to 10^2 Ω-cm with the decrease in SSD from 14 cm to 12 cm may cause due to the increment of the crystalline quality [38, 41]. After that, the resistivity gradually reduced and finally reached 10 Ω-cm as we further decreased the SSD to 8 cm. The film resistivity decreases due to crystallite

size increment [38] and improved film crystallinity and grain boundaries [41]. Generally, the resistivity decreases as the grain size increases [25, 26]. This reduction of film resistivity with SSD is consistent with previously published works [25-27, 42].

4. Conclusion

This work aims to investigate the optimum distance between the evaporation source and substrate for achieving the high quality of thermally evaporated CdS films. The XRD analysis of the as-deposited CdS films revealed the most preferential stable hexagonal wurtzite crystal structure orientation (002) with polycrystalline nature. The crystallographic properties of as-grown CdS films showed better quality as we decrease the SSD value to 8 cm. The better crystallinity is revealed at 10 cm distance. All the deposited CdS films transmitted the incident photon after the band edge of 500 nm wavelength. They exhibited an average transmittance of over 75%, which implies that the maximum amount of photon transmitting into the active region causes the increment of photogenerated current density in the solar cell device. The optical bandgap of as-deposited CdS thin films followed a decreasing trend from 3.44 eV to 3.37 eV as we decrease SSD from 14 cm to 8 cm. On the other hand, the carrier concentration of deposited CdS films increases from 3.78×10^{13} cm^{-3} to 4.4×10^{16} cm^{-3} with SSD decrement. Besides, the mobility and resistivity of the deposited CdS films decrease with the decrement of SSD. We prefer 10 cm SSD is suitable for growing CdS films in our case as this shows better structural, optical, and electrical properties.

Acknowledgement

This work has been supported by the Department of Electrical and Electronic Engineering of Chittagong University of Engineering and Technology, Bangladesh. The authors would like to acknowledge and appreciate the contribution of the Industrial Physics Division, BCSIR, Dhaka, and the Institute of Sustainable Energy, Universiti Tenaga Nasional, Malaysia, for their valuable suggestions and assistance in characterizing the deposited samples.

Nomenclature

CdS	Cadmium Sulfide
SSD	Source to Substrate Distance
XRD	X-ray diffraction
HEMS	Hall Effect Measurement System
CSS	Close-Spaced Sublimation
CBD	Chemical Bath Deposition
PLD	Plused Laser Deposition
TE	Thermal Evaporation
BSG	Borosilicate Glass
DI	Deionized Water
MAMD	Methanol, Acetone, Methanol, Deionized
Mo	Molybdenum

References

[1] Z. Fang, X. C. Wang, H. C. Wu, and C. Z. Zhao, "Achievements and challenges of CdS/CdTe solar cells," *Int. J. Photoenergy*, vol. 2011, no. 1, 2011. (Article)

[2] A. Tanushevski, and H. Osmani, "CdS thin films obtained by chemical bath deposition in presence of fluorine and the effect of annealing on their properties," *Chalcogenide Lett.* , vol. 15, no. 2, pp. 107-113, February 2018. (Article)

[3] Bhaskar Reddy Tetali, "Stability Studies of CdTe/CdS Thin Film Solar Cells," Ph. D. thesis, University of South Florida, USA., March 2005. (Ph. D. Thesis)

[4] R. S. Meshram, B. M. Suryavanshi, and R. M. Thombre, "Structural and optical properties of CdS thin films obtained by spray pyrolysis,"*Advances in Applied Science Research*, vol. 3 no. 3, pp. 1563-1571, 2012. (Article)

[5] X. Wu, "High-efficiency polycrystalline CdTe thin-film solar cells," *Solar Energy,* vol. 77, no. 6, pp. 803-814, December 2004. (Article)

[6] Mrinmoy Dey, Mahmudul Hasan, Rahat Amin, Maitry Dey, N. K. Das, A. K. Sen Gupta, M. A. Matin and N. Amin, "Design of Highly Efficient CdSe Solar Cell with CdS as Buffer Layer Material," *in Proceedings of the International Conference on Mechanical Engineering and Renewable Energy,* PI-387, 18-20 December, 2017, CUET, Chittagong, Bangladesh. (Conference Paper)

[7] S. Kasap, and P. Capper, *Springer Handbook of Electronic and Photonic Materials*, 2nd ed., Springer International Publishing, 2017, Chapter 16. (Book Chapter)

[8] Mrinmoy Dey, Ismad Ahmad Asha, Zarin Tasnim Smita, Maitry Dey and Nipu Kumar Das, "Highly Efficient ZnTe Solar Cell with PbTe BSF," *in Proceedings of the 5th International Conference on Advances in Electrical Engineering*, 26-28 September, 2019, Dhaka, Bangladesh. (Conference Paper)

[9] K. Ravichandran, and P. Philominathan, "Comparative study on structural and optical properties of CdS films fabricated by three different low-cost techniques," *Applied Surface Science*, vol. 255, no. 11, pp. 5736-5741, March 2009. (Article)

[10] Mrinmoy Dey, M. A. Matin, Nipu Kumar Das, and Maitry Dey, "Germanium Telluride as a BSF material for high efficiency ultra-thin CdTe solar cell," *in Proceedings of the 9th International Forum on Strategic Technology*, 21-23 October, 2014, Cox's Bazar, Bangladesh. (Conference Paper)

[11] Mrinmoy Dey, Maitry Dey, M. A. Matin, and Nowshad Amin, "Design of Highly Stable and Efficient Molybdenum Telluride PV Cells with Arsenic Telluride BSF," *in Proceedings of the 3rd International Conference on Electrical Engineering and Information & Communication Technology,* Dhaka, Bangladesh, 22-24 September, 2016. (Conference Paper)

[12] Mrinmoy Dey, M. A. Matin, and Maitry Dey, "Arsenic Telluride BSF for High Performance and Stable ultra-thin CdTe PV cell," *International Journal of Research in Computer Engineering and Electronics,* vol. 4, no. 2, July 2015. (Article)

[13] V. D. Moreno-Regino, F. M. Castañeda-de-la-Hoya, C. G. Torres-Castanedo, J. Márquez-Marín, R. Castanedo-Pérez, G. Torres-Delgado, and O. Zelaya-Ángel, "Structural, optical, electrical and morphological properties of CdS films deposited by CBD varying the complexing agent concentration," *Results in Physics*, vol. 13, June 2019. (Article)

[14] A. S. Z. Lahewil, Y. Al-Douri, U. Hashim, and N. M. Ahmed, "Structural and optical investigations of cadmium sulfide nanostructures for optoelectronic applications," *Sol. Energy*, vol. 86, no. 11, pp. 3234–3240, November 2012. (Article)

[15] N. H. Kim, S. H. Ryu, H. S. Noh, and W. S. Lee, "Electrical and optical properties of sputter- deposited cadmium sulfide thin films optimized by annealing temperature," *Mater. Sci. Semicond. Process.*, vol. 15, no. 2, pp. 125-130, April 2012. (Article)

[16] G. Pérez-Hernández, J. Pantoja-Enríquez, B. Escobar-Morales, D. Martinez-Hernández, L. L. Díaz-Flores, C. Ricardez-Jiménez, N. R. Mathews, and X. Mathew, "A comparative study of CdS thin films deposited by different techniques," *Thin Solid Films*, vol. 535, pp. 154–157, May 2013. (Article)

[17] Miguel A. Contreras, Manuel J. Romero, Bobby To, F. Hasoon, R. Noufi, S. Ward, and K. Ramanathan, "Optimization of CBD CdS process in high efficiency Cu(In,Ga)Se based solar cells," *Thin Solid Films*, vol. 403–404, pp. 204–211, February 2002. (Article)

[18] Sachin Rondiya, Avinash Rokade, Adinath Funde, Moses Kartha, Habib Pathan, and Sandesh Jadkar, "Synthesis of CdS thin films at room temperature by RF-magnetron sputtering and study of its structural, electrical, optical and morphology properties," *Thin Solid Films*, vol. 631, pp. 41–49, June 2017. (Article)

[19] A. A. Yadav, M. A. Barote, and E. U. Masumdar, "Studies on nanocrystalline cadmium sulphide (CdS) thin films deposited by spray pyrolysis," *Solid State Sciences*, vol. 12, no.7, pp. 1173-1177, July 2010. (Article)

[20] B. Ullrich, R. Schroeder, H. Sakai, A. Zhang, and S. Z. D. Cheng, "Two-photon-excited green emission and its dichroic shift of oriented thin-film CdS on glass formed by laser deposition," *Appl. Phys. Lett.*, vol. 80, no. 3, pp. 356–358, 2002. (Article)

[21] M. Thambidurai, N. Murugan, N. Muthukumarasamy, S. Agilan, S. Vasantha, and R. Balasundaraprabhu, "Influence of the Cd/S Molar Ratio on the Optical and Structural Properties of Nanocrystalline CdS Thin Films," *J. Mater. Sci. Technol.*, vol. 26, no. 3, pp. 193-199, March 2010. (Article)

[22] A. Ashour, N. El-Kadry, and S. A. Mahmoud, "On the electrical and optical properties of CdS films thermally deposited by a modified source," *Thin Solid Films*, vol. 269, no. 1-2, pp. 117-120, November 1995. (Article)

[23] S. Azmi, M. Nohair, M. El Marrakchi, E. Khoumri, and M. Dabala, "Effect of the Complexing Agents on the Properties of Electrodeposited CZTS Thin Films," *7th International Conference on Renewable Energy Research and Applications (ICRERA)*, pp. 1346-1351, 2018. (Conference Paper)

[24] Salah Abdul-Jabbar Jassim, Abbaker A. Rashid Ali Zumaila, and Gassan Abdella Ali Al Waly, "Influence of substrate temperature on the structural, optical and electrical properties of CdS thin films deposited by thermal evaporation," *Results in Physics*, vol. 3, pp. 173-178, August 2013. (Article)

[25] B. P. Singh, R. Kumar, A. Kumar, M. Kumar, and A. G. Joshi, "Vacuum thermal deposition of crystalline, uniform and stoichiometric CdS thin films in ambient H_2S atmosphere," *Indian Journal of Pure & Applied Physics*, vol. 55, pp. 463-470, July 2017. (Article)

[26] M. Devika, N. Koteeswara Reddy, D. Sreekantha Reddy, S. Venkatramana Reddy, K. Ramesh, E. S. R. Gopal, K. R. Gunasekhar, V. Ganesan, and Y. B. Hahn, "Optimization of the distance between source and substrate for device-grade SnS films grown by the thermal evaporation technique," *Journal of Physics: Condens. Matter,* vol. 19, no. 30, August 2007. (Article)

[27] L. Kai, L. Bingchi, H. Yudan, L. Wenqi, and L. Jiangshan, "Influence of the Source to Substrate Distance on the Growth, Tribological Properties and Optical Properties of Be Films," *Journal of Wuhan University of Technology-Mater Sci. Ed,* vol. 33, no. 2, pp. 320-325, April 2018. (Article)

[28] Maitry Dey, N. K. Das, and M. A. Matin, "Effect of Thermally Evaporated n-CdTe Thin Film on Homojunction CdTe Solar Cell," *in Proceedings of the 5th International Conference on Advances in Electrical Engineering*, Dhaka, Bangladesh, September 2019. (Conference Paper)

[29] N. K. Das, S. F. U. Farhad, J. Chakaraborty, A. K. S. Gupta, M. Dey, M. Al-Mamun, M. A. Matin, and N. Amin, "Structural and optical properties of RF-sputtered CdTe thin films grown on CdS:O/CdS bilayers," *International Journal of Renewable Energy Research*, vol. 10, no. 1, pp. 293-302, March 2020. (Article)

[30] Maitry Dey, N. K. Das, A. K. Sengupta, Mrinmoy Dey, M. S. Hossain, M. A. Matin, and N. Amin, "Deposition of CdS Thin Film by Thermal Evaporation," *in Proceedings of the 2nd International Conference on Electrical, Computer and Communication Engineering,* Cox's Bazar, Bangladesh, 07-09 February, 2019. (Conference Paper)

[31] T. Sivaraman, V. Narasimman, V. S. Nagarethinam, and A. R. Balu, "Effect of chlorine doping on the structural, morphological, optical and electrical properties of spray deposited CdS thin films," *Prog. Nat. Sci. Matter. Int.*, vol. 25, pp. 392-398, June 2015. (Article)

[32] E. M. K. Ikball Ahamed, N. K. Das, A. K. S. Gupta, M. N. I. Khan, M. A. Matin, and N. Amin "Structural and Optical Characterization of As-grown and Annealed $Zn_XCd_{1-x}S$ Thin-films by CBD for Solar Cell Applications," *International Journal of Renewable Energy Research*, vol. 10, no. 3, September 2020. (Article)

[33] N. M. Shah, J. R. Ray, M. S. Desai, and C. J. Panchal, "Influence of substrate temperature on structural, optical and electrical properties of evaporated cadmium sulphide thin films," *Journal of Optoelectronics and Advanced Materials,* vol. 12, no. 10, pp. 2052-2056, October 2010. (Article)

[34] M. A. Islam, M. S. Hossain, M. M. Aliyu, Y. Sulaiman, T. Razykov, K. Sopian, and N. Amin, "Structural, Optical and Electrical Properties of In Doped CdS Thin Films Prepared from Co-Sputtering Technique," *Latest Trends in Renewable Energy and Environmental Informatics*, pp. 155-160, 2013. (Article)

[35] Nafiseh Memarian, Seyeed Mohammad Rozati, Isabella Concina, and Alberto Vomiero, "Deposition of Nanostructured CdS Thin Films by Thermal Evaporation Method: Effect of Substrate Temperature," *Materials,* vol. 10, no. 3, pp.773-780, July 2017. (Article)

[36] Won-Jae Lee, James Sharp, Gilberto A. Umana-Membreno, John Dell, and Lorenzo Faraone, "Deposition Heating Effect on CdS Thin Films Prepared by Thermal Evaporation for CdTe Solar Cells," *in Proceedings of 3rd World Conf. on Optoelectronic and Microelectronic Materials & Devices*, pp. 153-155, Perth, WA, Australia, 14-17 Dec. 2014. (Conference Paper)

[37] Nabeel A. Bakr, Falah I. Mustafa, and Roaa J. Mohammed, "Structural, Optical and Electrical Properties of Thermally Deposited CdS Thin Films," *Journal of Chemical, Biological and* Physical Sciences, vol. 7, no. 4, pp. 881-889, September 2017. (Article)

[38] N. K. Das, J. Chakrabartty, S. F. U. Farhad, A. K. Sen Gupta, E. M. K. Ikbal Ahmed, K.S. Rahman, A.Wafi, A. A. Alkahtani, M. A. Matin, and N. Amin, "Effect of substrate temperature on the properties of RF sputtered CdS thin films for solar cell applications," *Results in Physics*, vol. 17, April 2020. (Article)

[39] S. Z. Werta, O. K. Echendu, F. B. Dejene, Z. N. Urgessa, and J. R. Botha, "Temperature-dependent properties of electrochemically grown CdS thin films from acetate precursor," *Appl. Phys. A Mater. Sci. Process.,* vol. 124, no. 9, August 2018. (Article)

[40] A. Ashok, G. Regmi, A. Remero-Nunez, M. Solis-Lopez, S. Velumani, and H. Castaneda "Comparative studies of CdS thin films by chemical bath deposition techniques as a buffer layer for solar cell applications," *Journal of Materials Science:materials in Electronics,* no. 10, February 2020. (Article)

[41] D. Kathirvel, N. Suriyanarayanan, S. Prabahar, and S. Srikanth, "Structural, electrical and optical properties of CdS thin films by vacuum evaporation deposition," *Journal of Ovonic Research,* vol. 7, no. 4, pp. 83-92, August 2011. (Article)

[42] F. H. Wang, and C. L. Chang, "Effect of substrate temperature on transparent conducting Al and F co-doped ZnO thin films prepared by rf magnetron sputtering," *Appl. Surf. Sci.,* vol. 370, pp. 83–91, 2016. (Article)